

## AERODYNAMICS OF HOVERING FLIGHT IN THE LONG-EARED BAT *PLECOTUS AURITUS*

By U. M. NORBERG

*Department of Zoology, University of Göteborg, Fack, S-400 33 Göteborg 33,  
Sweden*

(Received 22 March 1976)

### SUMMARY

Steady-state aerodynamic and momentum theories were used for calculations of the lift and drag coefficients of *Plecotus auritus* in hovering flight. The lift coefficient obtained varies between 3.1 and 6.4, and the drag coefficient between  $-5.0$  and  $10.5$ , for the possible assumptions regarding the effective angles of attack during the upstroke. This demonstrates that hovering flight in *Plecotus auritus* can not be explained by quasi-steady-state aerodynamics. Thus, non-steady-state aerodynamics must prevail.

### INTRODUCTION

Hovering flight is a common habit of the long-eared bat *Plecotus auritus*, which has crowns of broad-leafed trees as its main feeding habitat. It has a very agile and manoeuvrable flight and is even able to fly vertically up and down for short periods. It often flies very slowly and can therefore make sharp turns in narrow spaces. Hovering is a very power-demanding type of flight. It is consistent with steady-state aerodynamics in hummingbirds and a variety of insects (Weis-Fogh, 1972, 1973), but this is not so in some insects (Weis-Fogh, 1973; R. Å. Norberg, 1975) and the pied flycatcher (U. M. Norberg, 1975). Its aerodynamics has not been previously worked out in bats.

The purpose of this investigation is to find out if hovering flight in the long-eared bat, *Plecotus auritus*, is consistent with steady-state aerodynamics, or if it has to be explained by non-steady-state phenomena. The kinematics, aerodynamics, and energetics of slow horizontal flight in *P. auritus* can be explained by steady-state aerodynamics (Norberg, 1976). Previously obtained data for the kinematics of hovering flight in *P. auritus* (Norberg, 1970) have been used in the present analysis and evaluation of the aerodynamics of hovering flight in this species.

### MATERIAL AND METHODS

Body measurements and flight parameters for hovering flight are given in Table 1. Calculations are based on previously described data from a wing-stroke in hovering flight (Norberg, 1970) (Figs. 1 and 2).

The average force coefficients are estimated with the same method as for horizontal

Table 1. *Body measurements and flight parameters for hovering flight in Plecotus auritus*

Stroke angle, $\phi$	$120^\circ = 2.1 \text{ rad}$
Stroke frequency, $n$	$11.35 \text{ Hz}$
Angle of tilt of stroke plane, $\beta$	$30^\circ$
Induced wind, $V_i$	$0.80 \text{ m s}^{-1}$
Air density, $\rho$	$1.22 \text{ kg m}^{-3}$
Body weight, $W$	$0.0883 \text{ N}$
Wing area, $A$	$0.0123 \text{ m}^2$
Wing span, $b$	$0.270 \text{ m}$
Wing length, $R$	$0.124 \text{ m}$
Aspect ratio, $b^2/A$	$5.9$
Wing loading, $W/A$	$7.18 \text{ N m}^{-2}$
Flight muscle mass/body mass	$0.137^*$

\* Data from Betz (1958).

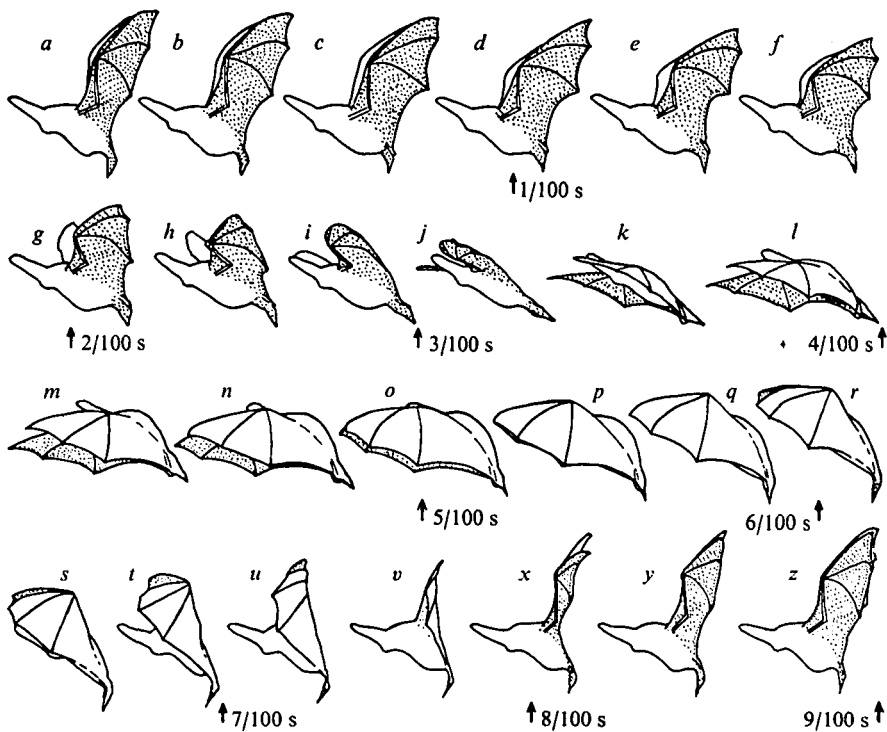


Fig. 1. The wing-movement cycle of *Plecotus auritus* in hovering flight, viewed from the side: a-m, downstroke; n-z, upstroke. (From Norberg, 1970.)

flight (Norberg, 1976). It involves the use of steady-state aerodynamic theory for calculation of average lift and drag coefficients. The magnitudes of the force coefficients thus derived are then used to judge the plausibility of the concept of steady-state aerodynamics in this state of flight. The average force coefficients obtained with this method of calculation must not exceed the maximum coefficients of lift and drag obtainable at the Reynolds number under which the wings operate, if steady-state

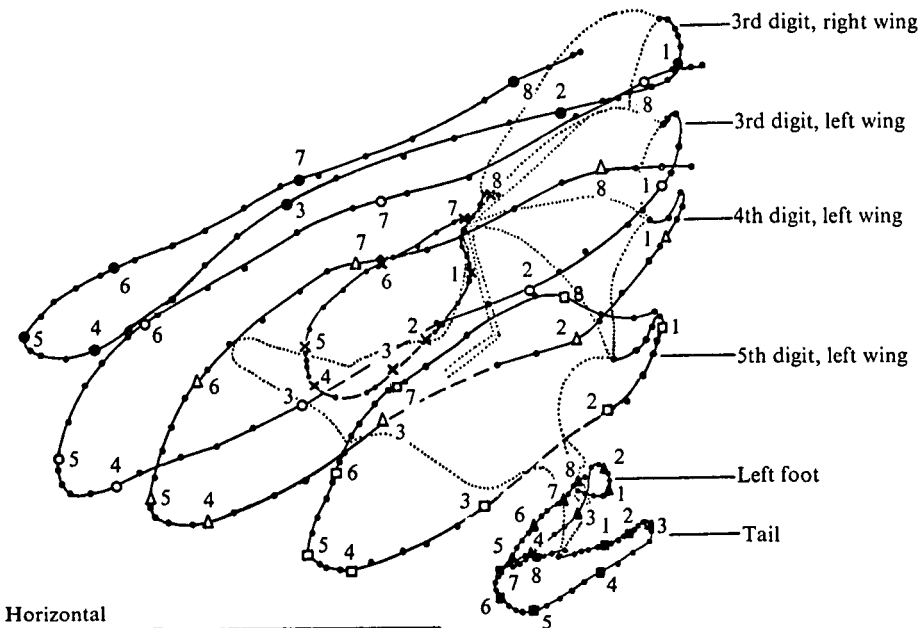


Fig. 2. Lateral projection of the movements of the wings, hind legs, and tail of *Plecotus auritus* in hovering flight. The tracks of different parts of the wings and tail are traced relative to the shoulder joint and long axis of the body. The uropatagium (tail membrane) is in its uppermost position when the wings are in about the middle of the downstroke. The numbers indicate each 100th of a second from the uppermost position of the wings. The figure is based on 42 frames (separated by *ca.* 2.1 msec). The positions as traced from the frames are indicated by dots. Figs. 1 and 2 are based on two different representative wing-strokes. (From Norberg, 1970.)

aerodynamics prevail. The method constitutes a further development of Weis-Fogh's (1972) formulae for calculation of  $C_L$  in hovering flight, and of Pennycuick's (1968) formulae for calculation of the resultant force coefficient in horizontal flapping flight. The new development results in an equation system expression from which the two average force coefficients,  $C_L$  and  $C_D$ , can be solved. The force coefficients thus obtained are the averages that actually prevail if steady-state aerodynamics prevails. Weis-Fogh calculated only the average lift coefficient and assumed a certain lift/drag ratio. He did not separate the upstroke and downstroke, but made calculations for half a downstroke and multiplied the value by 4, since hummingbirds and several insects have a rather symmetrical stroke. The hovering flight in *Plecotus* is unsymmetrical, i.e. the kinematics of the upstroke differs considerably from that of the downstroke. Hence, the upstroke and downstroke are treated separately in this investigation.

The general outline of the method (Norberg, 1976) is as follows. The sum of the vertical components  $L_{\text{vert}}(r, t)$  and  $D_{\text{vert}}(r, t)$  of the lift and drag forces, respectively, as integrated over the time of a whole wing-stroke and over the whole wings, must equal the weight,  $W$ , of the bat as integrated over the same time, and is

$$\int_{t=0}^{t=T} W dt = \int_{t=0}^{t=T} \left[ \sum_{r=1}^N (L_{\text{vert}}(r, t) + D_{\text{vert}}(r, t)) \right] dt, \quad (1)$$

where  $r$  denotes the spanwise distance from the fulcrum (humero-scapular joint) to the middle of a chordwise strip of the wing, and  $T$  denotes the time of a whole wing-stroke. The wing was divided in  $N$  chordwise strips, each 1 cm wide.

In the same way the sum of the integral of the horizontal components in the direction of the flight path,  $L_{\text{hor}}(r, t)$  and  $D_{\text{hor}}(r, t)$  of the lift and drag forces, respectively, must equal the time integral of the body drag of the bat. In hovering the body is immersed in the induced wind that probably is nearly vertical. The body therefore experiences a nearly vertical downward drag force, the horizontal component of which should be negligible. Therefore, the horizontal body drag is set equal to zero. Then,

$$0 = \int_{t=0}^{t=T} \left[ \sum_{r=1}^N (L_{\text{hor}}(r, t) + D_{\text{hor}}(r, t)) \right] dt. \quad (2)$$

Actually, the vertical component of the body drag force due to the induced wind should be added to  $W$  on the left side of equation (1). Since its magnitude is very small this force is also omitted.

$C_L$  and  $C_D$  enter the above two equations via  $L_{\text{vert}}(r, t)$ ,  $D_{\text{vert}}(r, t)$ ,  $L_{\text{hor}}(r, t)$ , and  $D_{\text{hor}}(r, t)$ , respectively, which are defined below. These two unknowns ( $C_L$  and  $C_D$ ) thus can be solved from equations (1) and (2).

The lift force,  $L(r, t)$ , and drag force,  $D(r, t)$  at a chordwise wing strip at distance  $r$  from the fulcrum, are

$$L(r, t) = \frac{1}{2} \rho V_R^2(r, t) A(r) C_L \quad (3)$$

and

$$D(r, t) = \frac{1}{2} \rho V_R^2(r, t) A(r) C_D, \quad (4)$$

where  $\rho$  is the air density,  $V_R(r, t)$  the resultant airspeed,  $A(r)$  the area of a strip at distance  $r$  from the fulcrum, and  $C_L$  and  $C_D$  the lift and drag coefficients, respectively.

To obtain the vertical components of these forces, one first has to project the forces to the vertical plane through and normal to the long wing-axis (fig. 13 in Norberg, 1976). Then, the true, vertical projection has to be found. The true vertical components then become

$$L_{\text{vert}}(r, t) = L(r, t) \cos \psi (1 - \cos^2 \gamma \sin^2 \beta)^{\frac{1}{2}} \quad (5)$$

and

$$D_{\text{vert}}(r, t) = D(r, t) \sin \psi (1 - \cos^2 \gamma \sin^2 \beta)^{\frac{1}{2}}, \quad (6)$$

where  $\psi$  is the angle between the incident air and the horizontal and  $\beta$  is the angle of tilt of the stroke plane.  $\gamma$  is the positional angle of the long wing-axis, measured in the stroke plane from the intersection below the bat between the stroke plane and a sagittal plane to the body through the wing hinge, and is

$$\gamma(t) = \bar{\gamma}(t) + \frac{1}{2} \phi \sin(2\pi n t), \quad (7)$$

where  $\bar{\gamma}(t)$  is the mean positional angle, and  $\phi$  the stroke angle.

The horizontal components of  $L(r, t)$  and  $D(r, t)$  in the flight path are estimated in the corresponding way, and are

$$L_{\text{hor}}(r, t) = L(r, t) \sin \psi \left( \frac{1 - \cos^2 \gamma}{1 - \cos^2 \gamma \sin^2 \beta} \right)^{\frac{1}{2}}, \quad (8)$$

and

$$D_{\text{hor}}(r, t) = D(r, t) \cos \psi \left( \frac{1 - \cos^2 \gamma}{1 - \cos^2 \gamma \sin^2 \beta} \right)^{\frac{1}{2}}. \quad (9)$$

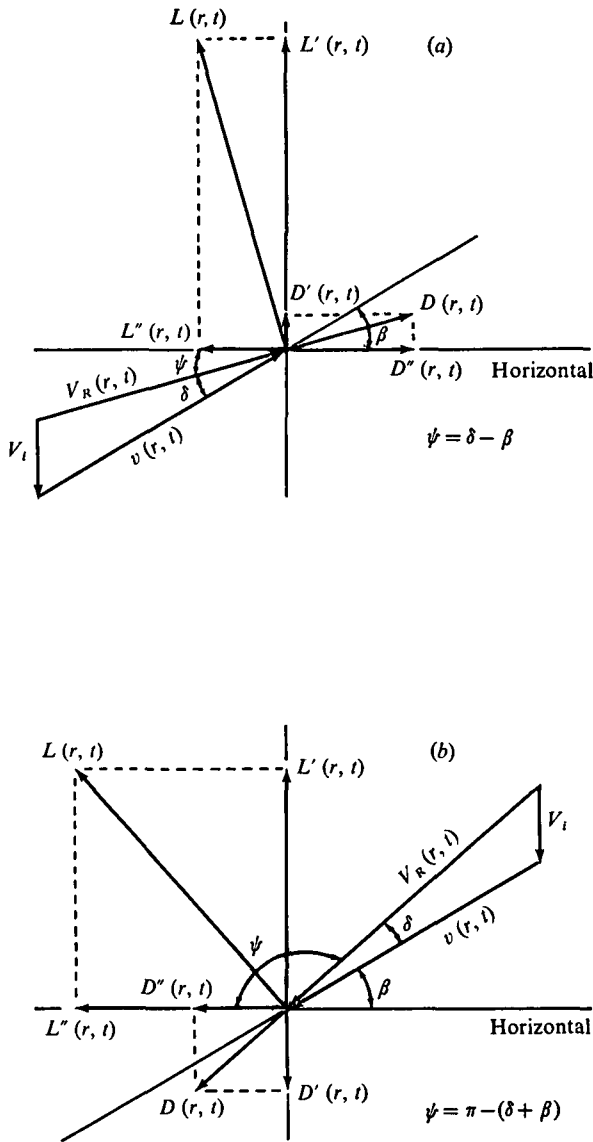


Fig. 3. Velocities ( $V$  and  $v$ ) at, and forces ( $L$  and  $D$ ) acting on, a chordwise wing-segment at a distance  $r$  from the fulcrum (wing hinge) in hovering flight.

(a) Downstroke. The wing section is not indicated but the effective angle of attack is positive.

(b) Upstroke. The air meets the dorsal side of the wing and the effective angle of attack is negative.

Positive sign denotes a forwardly directed force; negative sign, a backwardly directed force.

The instantaneous resultant velocity  $V_R(r, t)$  is the resultant of the flapping speed and the induced velocity. The movement of the long wing-axis is almost sinusoidal with respect to angular displacement. Therefore, the flapping velocity of a wing-

element at distance  $r$  from the fulcrum can be conveniently approximated with the equation for simple harmonic motion,

$$v(r, t) = r\pi\phi n \cos(2\pi nt), \quad (10)$$

where  $n$  is the stroke frequency.

The air is assumed to be accelerated vertically downwards. The induced velocity is assumed to be constant and uniformly distributed over a  $360^\circ$  disc with the wing span as diameter during the entire wingstroke, though there might be fluctuations in the downstroke and upstroke. According to the momentum theorem for an ideal actuator disc, the induced velocity at the level of the disc then becomes

$$V_i = \left( \frac{W}{2\rho S_d} \right)^{\frac{1}{2}}, \quad (11)$$

where  $S$  is the disc area.

From Fig. 3(a) and (b) it can be seen that the resultant airspeed during the downstroke is

$$V_R(r, t)^2 = v(r, t)^2 + V_i^2 - 2v(r, t)V_i \sin \beta, \quad (12)$$

and during the upstroke

$$V_R(r, t)^2 = v(r, t)^2 + V_i^2 + 2v(r, t)V_i \sin \beta. \quad (13)$$

Angle

$$\psi = \delta - \beta \quad (14)$$

during the downstroke, and

$$\psi = \pi - (\delta + \beta) \quad (15)$$

during the upstroke, where

$$\sin \delta = V_i \cos \beta / V_R(r, t). \quad (16)$$

#### Procedure

The wing was divided into three chordwise sections (I-III, Fig. 4) and the area of each was measured. The arm wing (the part of the wing proximal to the fifth digit) is flexed during the upstroke, thereby reducing the wing area. The area of the arm wing was estimated from my films and photographs to be reduced during the upstroke to *ca.* 65 % of the area of the extended arm wing, and at the reversal points to *ca.* 80 %. The hand wing (the part of the wing distal to the fifth digit) was not reduced at all during the upstroke, nor at the reversal points. The hand wing thus is maintained fully extended during the entire wing-stroke during hovering, as well as forward flight.

The indices of the horizontal and vertical components of the lift and drag forces were calculated from equations (5-8) for each of the three sections for 13 time-equidistant positions during the downstroke, and 13 during the upstroke. The time of the downstroke is longer than that for the upstroke. This has been taken into account when calculating the stroke frequency and flapping speed used here. The force coefficients were then obtained from equations (1) and (2).

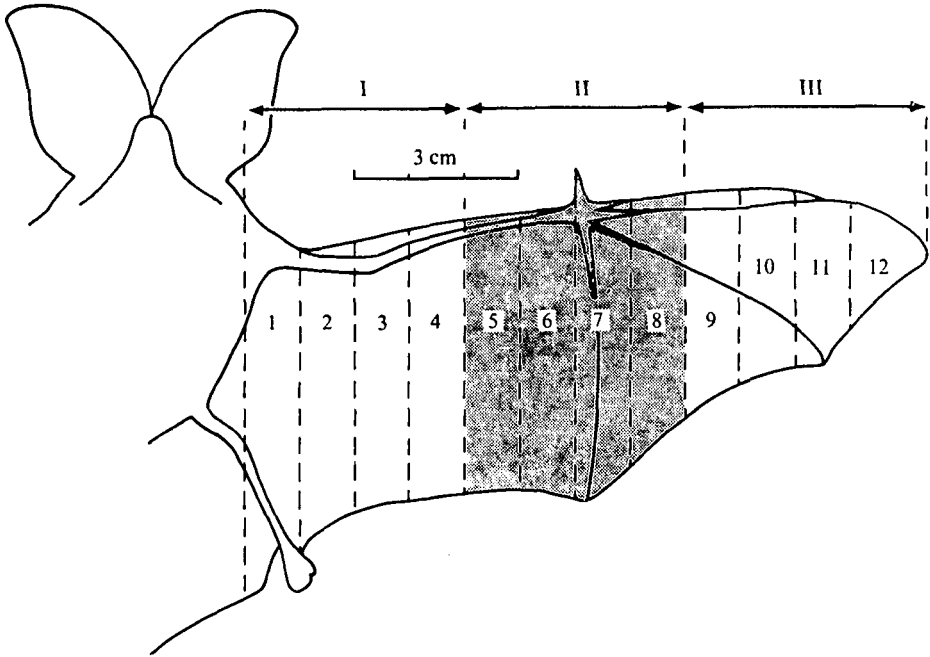


Fig. 4. The bat's outstretched wing divided into 12 strips, making up three sections (I-III) which are used for calculations of the force coefficients. (From Norberg, 1976.)

#### RESULT AND DISCUSSION

The virtual force index curves for the vertical and horizontal components of the lift and drag forces are shown in Figs. 5 and 6, respectively. The sum of the areas between the  $L_{\text{vert}}$  index curve and the abscissa, and between the  $D_{\text{vert}}$  index curve and the abscissa, in Fig. 5, times  $C_L$  and  $C_D$ , respectively, must equal the area under the horizontal hatched line for the weight (cf. equation (1)). The areas between the  $L_{\text{hor}}$  index curve and the abscissa and between the  $D_{\text{hor}}$  index curve and the abscissa, in Fig. 6, times  $C_L$  and  $C_D$ , respectively, must equal zero (cf. equation (2)).

Fig. 7 shows the inclinations of the wing chords (the lines joining the leading and trailing edges of given sections of the wing), relative to the horizontal, at  $0.20R$ ,  $0.50R$ , and  $0.85R$ . It was difficult to obtain reliable values from the tracings from the film for these inclinations of the different strips. For strips 3, 7 and 11, however, there are some reference points (elbow, thumb, finger joint and tips) (cf. Fig. 4). These strips were considered to be representative for the proximal (section I), middle (section II), and distal (section III) parts, respectively, of the wing. Only a rough estimate of the inclinations could be made from the film. However, it is clear that the angle between wing chord and the horizontal is positive for every section of the wing for every position of the entire wing-stroke.

During the downstroke, except at the reversal points, the relative wind is meeting the wing from a direction below the horizontal (Fig. 8). Therefore, the effective angles of attack (angles between the relative wind and zero-lift lines (Fig. 8) of the wing sections) are positive for every section of the wing during the entire downstroke, except at the reversal points, where they seem to be negative. During the upstroke

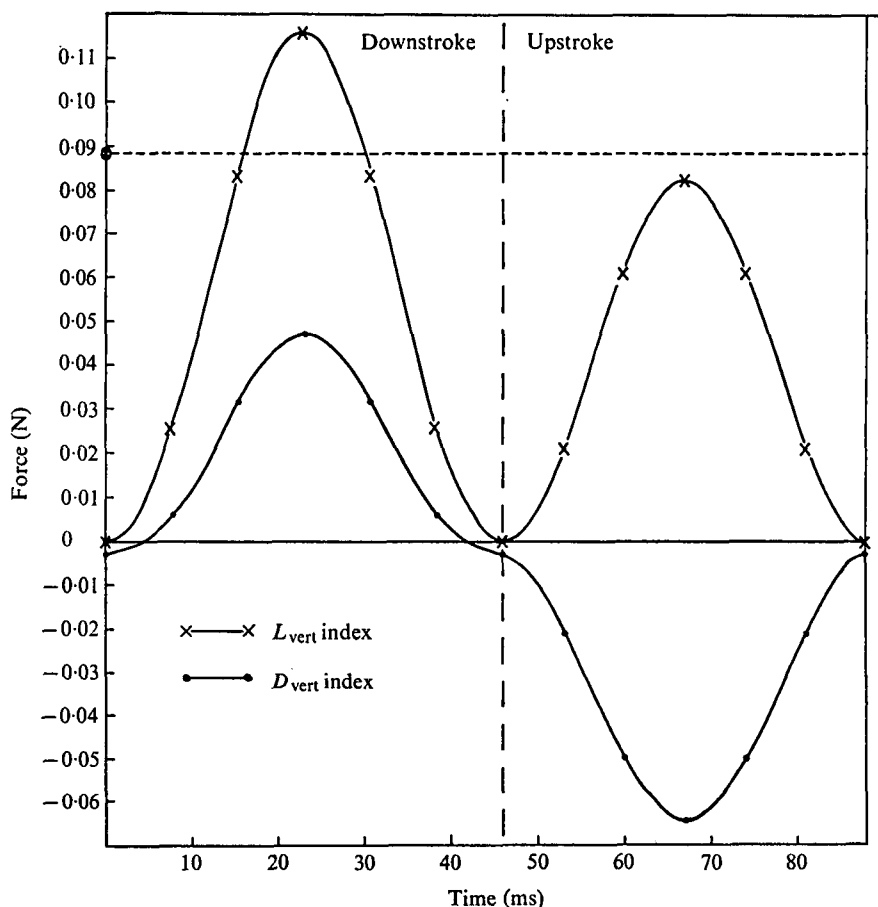


Fig. 5. The virtual force indices for the vertical components,  $L_{\text{vert}}$  and  $D_{\text{vert}}$ , of the lift and drag forces, respectively, plotted against time. The area under the  $L_{\text{vert}}$  curve, multiplied by the lift coefficient, plus the area under the  $D_{\text{vert}}$  curve, multiplied by the drag coefficient, must equal the body weight of the bat as integrated over the whole wing-stroke. The weight is indicated by a crossed circle on the ordinate and by a hatched horizontal line.

they seem to be negative in most phases, but positive for the distal section of the wing in at least one phase (cf. Fig. 8). The sign of the effective angles of attack during the upstroke depends on the size of the zero-lift angle (angle between wing chord and zero-lift line). Since the zero-lift angle is not known we must consider all possible alternative cases regarding the effective angles of attack during the upstroke. Hence, calculations are made under the following alternative assumptions.

(1) If one assumes that all effective angles of attack are negative for all sections of the wing during the entire upstroke, which they are during most of the upstroke, then the force coefficients would need to be  $C_L = 3.2$  and  $C_D = 10.5$  (Figs. 5 and 6). These are unreasonable values if steady-state aerodynamics prevails.

(2) If the effective angles of attack are positive at section III of the wing in two phases of the upstroke, which is uncertain but estimated from the film (cf. Fig. 8), then  $C_L$  becomes 5.0 and  $C_D$  5.8.

(3) The estimated angles between wing chord and relative wind are high during

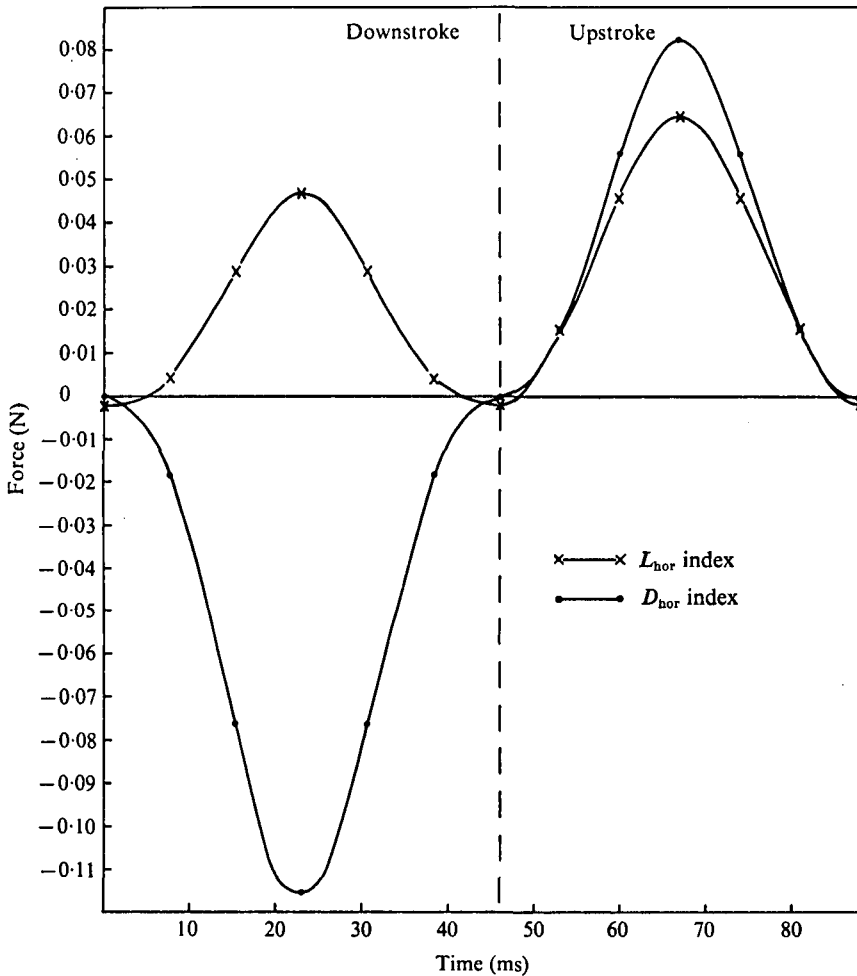


Fig. 6. The virtual force indices for the horizontal components,  $L_{hor}$  and  $D_{hor}$ , of the lift and drag forces, respectively, plotted against time. The area under the  $L_{hor}$  curve, multiplied by the lift coefficient, plus the area under the  $D_{hor}$  curve, multiplied by the drag coefficient, must equal zero in hovering flight.

most of the wing-stroke (Fig. 8), and so are therefore the effective angles of attack. If one assumes that the high angles of attack give only drag and thus zero lift, the lift force, as averaged over the entire wing-stroke, would become very small, which means that enough lift would not be produced for the bat to be able to fly. If the lift forces are assumed to become zero during the upstroke only and the drag force therefore being assumed to be reduced by 40%, the force coefficients become  $C_L = 3.1$  and  $C_D = 1.9$ ; and thus  $L/D = 1.6$ . These values might be the most probable ones. The 40% reduction of the drag is adopted from Pennycuik's (1971) wind-tunnel studies on *Rousettus* in gliding flight.

(4) If all effective angles of attack are positive during the upstroke,  $C_L$  would need to take the value 6.4 and  $C_D = 5.0$ , which are impossible values if steady-state aerodynamics prevails.

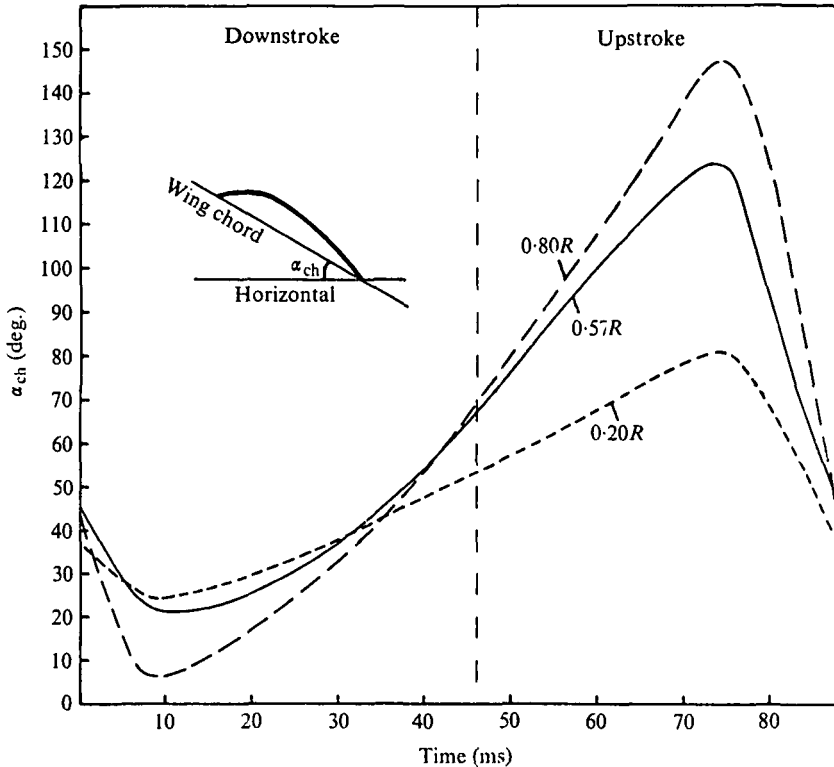


Fig. 7. Wing chord angles, relative to the horizontal ( $\alpha_{ch}$ ) at three chordwise positions of the wing at radial distances  $0.20R$ ,  $0.50R$ , and  $0.85R$ , respectively, from the wing hinge (corresponding to the middle of strips 3, 7 and 11, respectively) plotted against time for the bat in hovering flight. Based on film data.

Taking into account the above alternatives, which cover all possibilities, the calculations based on quasi-steady-state aerodynamics thus result in values for the force coefficients which are not consistent with quasi-steady-state aerodynamics. Thus, non-steady-state aerodynamics must prevail, and another approach must be taken to explain the hovering flight.

Weis-Fogh (1973) devised a generalized, quick method to calculate the lift coefficient in hovering animals. To get the corresponding drag coefficient, and hence  $L/D$  ratio, he used experimental lift/drag diagrams of aerofoils of suitable form and aspect ratio, so his drag coefficient refers to stiff aerofoils and not to the actual wing. The lift/drag ratio he used for *Plecotus* was 6.5. He further assumed that the wing-stroke was symmetrical as in hummingbirds. With data from Norberg (1970), i.e. the same set of kinematic data as used here, he then calculated the average coefficient of lift to be 1.3. From this result he drew the conclusion that hovering flight in *Plecotus* can be explained mainly by steady-state aerodynamics. However, the wing-stroke in *Plecotus* hovering flight is unsymmetrical, so the upstroke has to be treated separately.

Slow horizontal flight ( $2.35 \text{ m s}^{-1}$ ) can be explained by quasi-steady-state aerodynamics (Norberg, 1976). It is presumable that the lower the flight speed is, the larger the relative importance becomes of non-steady-state aerodynamics in force

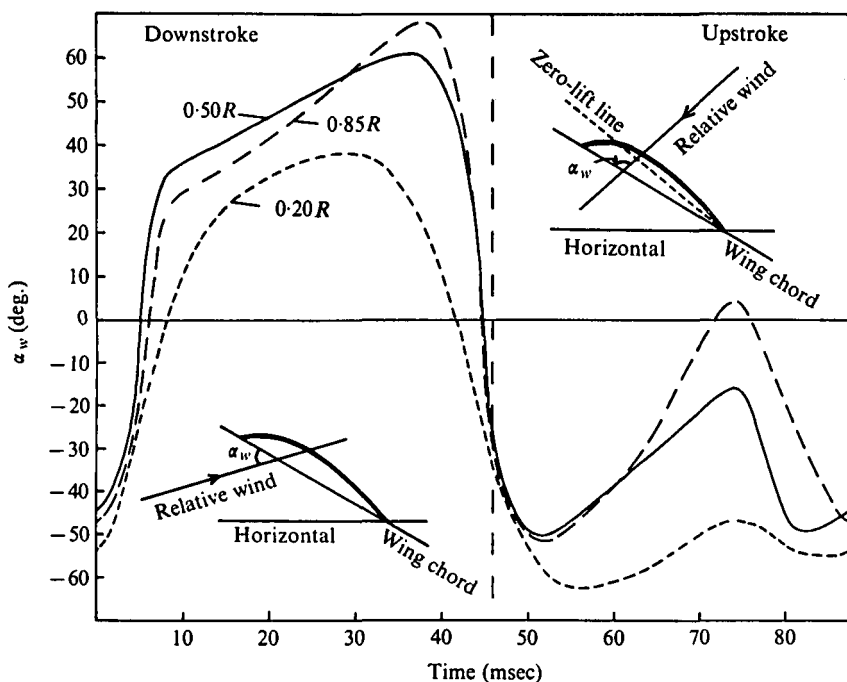


Fig. 8. The angles between wing chord and relative wind ( $\alpha_w$ ) at three chordwise positions of the wing (at radial distances 0.20R, 0.50R, and 0.85R, respectively, from the wing hinge) plotted against time for the bat in hovering flight. Based on film data. The zero-lift line is indicated arbitrarily in the inset figure on top right. The angle between this line and the wing chord, the zero-lift angle, is not known.

generation. In hovering, most or all of the vertical forces have to be explained by non-steady-state mechanisms.

I am indebted to Professor T. Eeg-Olofsson, Chalmers University of Technology, Göteborg, for making available a high-speed film camera, and to Civ.-ing. K. Pehrsson and Ing. R. Nilsson, Chalmers University of Technology, for filming aid. I also thank Dr C. J. Pennycuik, Department of Zoology, University of Bristol, for valuable comments upon the paper.

#### REFERENCES

- BETZ, E. (1958). Untersuchungen über die Korrelation der Flugmechanismen bei den Chiropteren. *Zool. Jb. (Abt. Anat.)* **77**, 491-526.
- NORBERG, R. A. (1975). Hovering flight of the dragonfly. *Aeschna juncea*. In *Swimming and Flying in Nature*, vol. 2 (ed. T. Y.-T. Wu, C. J. Brokaw and C. Brennen), pp. 763-81. Plenum Publ. Corp., N.Y. (Proc. Symp. on Swimming and Flying in Nature).
- NORBERG, U. M. (1970). Hovering flight of *Plecotus auritus* Linnaeus. *Bijdr. Dierk* **40**, 62-6 (Proc. 2nd Int. Bat. Res. Conf.).
- NORBERG, U. M. (1975). Hovering flight of the pied fly-catcher, *Ficedula hypoleuca*. In *Swimming and Flying in Nature*, vol. 2 (ed. T. Y.-T. Yu, C. J. Brokaw and C. Brennen), pp. 869-81. Plenum Publ. Corp. N.Y. (Proc. Symp. on Swimming and Flying in Nature).
- NORBERG, U. M. (1976). Kinematics, aerodynamics, and energetics of horizontal flapping flight in the long-eared bat *Plecotus auritus*. *J. exp. Biol.* (in the Press).
- PENNYCUICK, C. J. (1968). Power requirements for horizontal flight in the pigeon *Columba livia*. *J. exp. Biol.* **49**, 527-55.

- PENNYCUICK, C. J. (1971). Gliding flight of the dog-faced bat *Rousettus aegyptiacus* observed in a wind tunnel. *J. exp. Biol.* **55**, 833-45.
- WEIS-FOGH, T. (1972). Energetics of hovering flight in hummingbirds and in *Drosophila*. *J. exp. Biol.* **56**, 79-104.
- WEIS-FOGH, T. (1973). Quick estimates of flight fitness in hovering animals, including novel mechanisms for lift production. *J. exp. Biol.* **59**, 169-230.